Supporting Information

Glucose-responsive cascaded nanocatalytic reactor with self-modulated tumor microenvironment for enhanced chemo-catalytic therapy

Linqiang Mei,[a] Dongqing Ma,[a] Qin Gao,[a] Xiao Zhang,[a] Wenhui Fu,[a] Xinghua Dong,[a] Gengmei Xing,[a] Wenyan Yin,[a]* Zhanjun Gu,[a,b]* and Yuliang Zhao[c,d]

[a] CAS Key Laboratory for Biomedical Effects of Nanomaterials and Nanosafety, Institute of High Energy Physics, Chinese Academy of Sciences, Beijing 100049, China

[b] College of Materials Science and Optoelectronic Technology, University of Chinese Academy of Sciences, Beijing 100049, China

[c] CAS Center for Excellence in Nanoscience, National Center for Nanoscience and Technology of China, Chinese Academy of Sciences, Beijing 100190, China

[d] GBA Research Innovation Institute for Nanotechnology, Guangdong 510700, China

*Corresponding author: zjgu@ihep.ac.cn; yinwy@ihep.ac.cn

Experimental Section

Materials: Sodium molybdate (Na_2MoO_4, 99%), L-Cysteine (98%), chitosan (CS), and terephthalate (TA) were purchased from Alfa Aesar Ltd. Glucose oxidase (GOx) and glucose were purchased from MP Biomedicals. Tirapazamine (TPZ) was bought from Sigma-Aldrich. Nitric acid (HNO_3, 70%, BV-Ⅲ grade), ethanol, and hydrogen peroxide (H_2O_2) were purchased from Beijing Chemical Corporation. 3,3',5,5'-Tetramethylbenzidine (TMB) was obtained from Tokyo Chemical Industry. Fetal bovine serum (FBS) was provided by Gibco Company. Dulbecco′s modified Eagle′s medium (DMEM) and Roswell Park Memorial Institute 1640 medium (RPMI-1640) were purchased from HyClone Company, USA. Cell Counting Kit-8 (CCK-8) and Calcein-AM/propidium iodide (CA/PI) were purchased from Dojindo Laboratories, Japan. Hoechst 33342, 2′,7′-dichlorofluorescein diacetate (DCFH-DA) and GSH/GSSG Assay Kit were purchased from Beyotime Biotechnology Company. 8-Amino-5-chloro-7-phenylpyrido[3, 4-d]pyridazine-1,4 (2H, 3H) dione (L-012) was obtained from Wako Pure Chemical Industries, Ltd (Osaka, Japan). γ-H2AX antibodies, Hypoxia inducible factor-1α (HIF-1α) and Nitro-tyrosine antibodies were obtained from Abcam Company (USA). Deionized (DI) water was filtrated using a Millipore Milli-Q water system, USA.

Synthesis of MoS_2 and MoS_2@C. 100 mg of Na_2MoO_4 and 200 mg of L-Cysteine were added to round-bottom beaker containing 30 mL of DI water. Then, 0.1 M of HCl was added to adjust the pH to 5.61, and subsequently transferred to Teflon vessel autoclave. After reaction for 24 h at 200 °C, the solution was cooled to room

temperature. The MoS_2 NSs were obtained by centrifugation and washed with water, finally lyophilized for further use. Then, 30 mg of MoS_2 NSs were added to 60 mL of 1% CS solution. After sonification for 15 min, the solution was magnetically stirred for 18 h in the dark. To obtained pure MoS_2@C NSs, the solution was washed several times and centrifuged. Finally, the MoS_2@C NSs were lyophilized and stored at 4 ℃ for further use.

Synthesis of MoS_2@CG, and MoS_2@CGTC NCR. 25 mg of MoS_2@C NSs were dispersed in 20 mL of mixture solution containing 15 mg of GOx stirring for 12 h in the dark. The MoS_2@CG NSs was obtained and washed three times with water. To obtain MoS_2@CS-GOx-TPZ@CS (MoS_2@CGTC NCR), 1 mL of TPZ (4 mg mL^{-1}) was added into a 10 mL mixture solution of MoS_2@CG (1 mg mL^{-1}) in dark. After stirring for 24 h, the MoS_2@CGT was extracted and washed with DI water by centrifugation to remove the excess of TPZ. And then, the precipitate was added into a 20 mL of 1% CS solution and stirred for 24 h. Finally, the MoS_2@CGTC NCR was obtained after washing with water.

Characterization. Transmission electron microscope (TEM) and filed-emission scanning electron microscope (FE-SEM) images were obtained by JEM-2100Plus TEM and Hitachi S-4800, respectively. X-ray diffraction (XRD) analysis was carried out by Bruker D8 with Cu Kα radiation (λ = 1.5418 Å). Zeta potential and dynamic light scatting (DLS) analyses were taken by Nano-ZS90 (Malvern). The UV-Vis absorption spectra were acquired by a Hitachi U-3900 spectrophotometer (Japan). X-ray photoelectron spectroscopy (XPS) analysis was collected on an ESCALab220i-XL.

Raman spectra were obtained using a Renishaw Micro-Raman spectroscopy system (Renishaw in via plus). Fourier-transform infrared (FT-IR) spectra were recorded by Thermo Fisher spectrometer (Nicolet iN10). The thermogravimetric analysis (TGA, Q50) was performed to calculate the ratio of GOx loaded on the MoS_2@C surface.

Measurement of catalytic capacity of GOx, dissolved O_2 and H^+ generation. The catalytic activity of free GOx and MoS_2@CGTC NCR was detected by measuring the dissolved O_2 and pH changes in glucose solution. The glucose (500 μg mL^{-1}) was added to MoS_2@CGTC NCR (200 μg mL^{-1}) and free GOx solution (10 μg mL^{-1}), respectively. Meanwhile, the dissolved O_2 changes were detected by a dissolved oxygen meter (JPSJ-605F), and the pH value of the mixture was measured by a pH meter. Moreover, in order to verify the promoting effect of MoS_2@CGTC to GOx catalytic activity, comparative catalytic activity experiment of free GOx and MoS_2@CGTC were detected under same condition with prolonged incubation time in the presence of glucose. The catalytic activity of GOx was evaluated by recording the H_2O_2 generation with titanium oxysulfate ($TiOSO_4$) as the indicator. To further evaluate the effect of pH values on the catalytic production of H_2O_2, GOx (10 μg mL^{-1}) was firstly incubated with phosphate buffer (pH = 2~8) at room temperature for 2 h, followed by adding glucose (1.0 mg mL^{-1}) and incubating at room temperature for 30 min. Then, $TiOSO_4$ was added into above solution and incubated for 30 min. Finally, the absorbance value of sample at 412 nm was measured by a microplate reader.

The catalytic activity of MoS_2@CGTC NCR. A TMB-H_2O_2 double substrate system was performed to evaluate the peroxidase-like catalytic performance of

MoS_2@CGTC NCR. In a typical reaction, 300 μL of MoS_2@CGTC NCR (100 μg mL^{-1}) and 300 μL of glucose (0.5, 0.75, 1.5, 2.5, 5, 10, 15, 20, and 30 μg mL^{-1}) were added to 300 μL of TMB (1.0 mM) solution, respectively. Then, 0.1 mM of HAc-NaAc buffer solution (pH 4.5) was added and fixed the volume to 3.0 mL. After that, the mixture was shaken for different times in the dark. By regulating the pH and temperature to confirm the optimal condition. Besides, the Michaelis-Menten kinetic assay of MoS_2@CGTC NCR was examined by changing the concentration of TMB (0.167 mM to 1.0 mM) and H_2O_2 (0 mM to 3.0 mM), respectively. Subsequently, the absorbance spectrum at 650 nm was recorded by UV-Vis absorption spectrophotometer. Finally, the kinetic parameters were obtained using the Equation 1 and 2.

$$v_0 = \frac{V_{max} + [S]}{K_M + [S]} \qquad \text{Equation (1)}$$

$$\frac{1}{v_0} = \frac{K_m}{V_{max}} \cdot \frac{1}{[S]} + \frac{1}{V_{max}} \qquad \text{Equation (2)}$$

Where v is the initial velocity, K_m represents the Michaelis-Menten constant, V_{max} is the maximal reaction velocity and [S] is the concentration of substrate.

Detection of ·OH *in vitro*. The peroxidase-like catalytic generation of ·OH by MoS_2@CGTC NCR was evaluated using the terephthalate acid (TA), which can form 2-hydroxy-terephthalate acid (TAOH) with ·OH. 300 μL of TA (5 mM) was added in 300 μL of PBS, H_2O_2 (1 mM), MoS_2@CGTC (10 μg/mL), H_2O_2 + MoS_2@CGTC, or MoS_2@CGTC + glucose (5 mM), respectively. All the mixtures were shaken at 37 °C and kept in the dark at for 12 h. Finally, the fluorescence spectrum was recorded by fluorescence spectrometer.

Ellman's assay of GSH. 5,5′-dithiobis (2-nitrobenzoic acid) (DTNB), a typical Ellman reagent, can split the disulfide bond (-S-S-) to yield a yellow product. Briefly, 225 μL of MoS_2@CGTC NCR (50 mM BBS, 100 μg mL^{-1}) was added into 225 μL of GSH solution (1.0 mM). The GSH solution and GSH mixed with H_2O_2 (1.0 mM) solution were set as negative control group and positive control group, respectively. The mixtures were incubated at 25 or 37 °C for different time (0.5, 2, 4, 6, and 8 h), while shaking at 150 rpm. Next, 15 μL of DTNB solution (100 mM) and 785 μL of Tris-HCl (5 mM) were added into above solution. Subsequently, after centrifugation the absorbance of supernatant at 410 nm was measured by a Multiskan MK3 microplate spectrophotometer (Thermo fisher Scientific).

Detection of GSH/GSSG ratio. The GSH/GSSG ratio was further evaluated by GSH/GSSG assay kit (Beyotime). Firstly, 225 μL of MoS_2@CGTC NCR (100 μg mL^{-1}) was added into 225 μL of GSH solution (1.0 mM), and incubated at 37 °C for different time (0.5, 2, 4, and 6 h), while shaking at 150 rpm. Then, 90 μL of GSH removal solution M was added into above solution. After vortex sufficiently, the mixed solutions were further incubated for 1 h. Subsequently, the absorbance of supernatant at 410 nm was measured after centrifugation. Finally, the supernatant was used for GSH and GSSG assay, and GSH/GSSG was detected according to the manufacturer's instructions.

Cellular culture. Human lung adenocarcinoma cells (A549) and Human umbilical vein endothelial cells (HUVEC) were cultured in RPMI-1640 and DMEM medium

supplemented with 1% penicillin/streptomycin, 10% FBS at 37 ºC in a humidified atmosphere with 5% CO_2, respectively.

Cellular uptake. A549 cells (1×10^5 cells/well) were planted in six-well plates and incubated for 24 h. After that, the cells were incubated with 50 μg mL^{-1} of MoS_2@C were added and incubated for different times (0 h, 6 h, and 12 h). After washed three times with PBS, cells were fixed with 4% paraformaldehyde for 10 min, stained with Hoechst 33342 for 20 min, and finally washed with PBS. Subsequently, the cell images were observed by an IX73 inverted fluorescence microscope with a highly numerical dark-field condenser.

***In vitro* cytotoxicity.** Cell viability was evaluated by a standard CCK-8 assay. Briefly, HUVEC and A549 cells were cultured in 96-well plates (8×10^3 cells per well) for 24 h, followed by replacement with medium containing different concentrations of MoS_2@C, MoS_2@CG or MoS_2@CGTC NCR (0, 3.125, 6.25, 12.5, 25, 50, 100, and 200 μg mL^{-1}). The cells were washed three times with PBS. Then, 100 μL of CCK-8 (10%) fresh culture medium was added and incubated for 40 min. Finally, relative cell viability was calculated using the absorbance value at 450 nm by a microplate reader.

Detection of GSH/GSSG ratio *in vitro*. A549 cells were incubated in 6-well plate at a density of 1×10^5 cells/well for 24 h and then incubated with different concentrations of MoS_2@CGTC NCR (0, 2.5, 5, 10, 20, and 40 μg/mL) for 12 h. The cells were collected by centrifugation at 12000 rpm for 5 min at 4 °C and added with 3 × protein solution M. After sufficient vortex, the mixed solutions were frozen and thawed twice using liquid nitrogen and 37 °C water bath, respectively. The samples

were placed at 4 °C for 5 min and then centrifuged at 10 000 rpm for 10 min at 4 °C. Finally, the supernatant was used for GSH and GSSG assay, and GSH/GSSG was detected according to the manufacturer's instructions.

***In vitro* synergistic antitumor effect.** *In vitro* synergistic antitumor effect was assayed by a CCK-8 assay, Calcein-AM (CA) and propidium iodide (PI) staining, Annexin V-FITC/PI apoptosis and necrosis assay, comet assay, and Bio-TEM assay, respectively. For CCK-8 assay, A549 cells were seeded in 96-well plates and cultured for 24 h. Then, the culture medium was replaced with different concentrations of MoS_2@CG (0~100 μg mL^{-1}) or MoS_2@CGTC NCR (0~100 μg mL^{-1}) solution in the different culture medium (high glucose and low glucose) and normoxia/hypoxia culture condition. After 6 h of co-incubation, the culture medium was replaced by CCK-8 solution. Finally, the absorbance at 450 nm of the supernatant was recorded by a microplate reader. For CA and PI staining, A549 cells were seeded in 6-well plates (5×10^4 cells per well) for 24 h, followed by replacement with different concentrations of the MoS_2@C, MoS_2@CG or MoS_2@CGTC NCR and co-incubation for another 12 h. After different treatments, the cells were stained with the CA and PI solution, and observed by Nikon A1 confocal laser scanning microscope (CLSM). Next, the cells apoptosis/necrosis was evaluated by an annexin V-FITC/PI double staining through flow cytometry (Accuri c6, BD, USA). 2×10^5 of A549 cells were incubated in 6-well plates for 24 h. Afterward, the cells were divided into four groups: Control, MoS_2@C (100 μg mL^{-1}), MoS_2@CG (100 μg mL^{-1}) and MoS_2@CGTC NCR (100 μg mL^{-1}), and co-incubated for 6 h, respectively. Then, the cells were collected by trypsinization and

centrifugation. After dyed with Annexin V-FITC/PI kit, the cells were detected by flow cytometry.

Intracellular ·OH detection. The intracellular ·OH was detected using ·OH specific indicator Mitochondrial Hydroxyl Radical Detection Assay (OH580, Abcam). The A549 cells (10^5 cells per well) were cultured for 24 h, and then the culture medium was replaced with MoS_2@C, MoS_2@CG, and MoS_2@CGTC in glucose-free RPMI 1640 medium, respectively. After incubation for another 4 h, the cells were washed three times with PBS. Next, 200 μL of OH580 working solution was added into each group for further incubation for 1 h. Subsequently, the cells were washed with PBS for three times and cell nucleus were stained with Hoechst 33342 for another 20 min. Finally, the cells were washed with PBS for three times and observed by the Nikon A1 confocal laser scanning microscope (CLSM). In addition, the total amount of ROS in A549 cells was further detected using 2,7-dichlorodihydrofluorescein diacetate (DCFH-DA). The A549 cells (8×10^5 cells per well) were cultured for 24 h in 24-well plates. Then the culture medium was replaced with MoS_2@C, MoS_2@CG, and MoS_2@CGTC in glucose-free RPMI 1640 medium, respectively. After another 4 h, the cells were washed three times with PBS. Next, 5 μM of DCFH-DA was added into each group for further incubation for 30 min. Finally, the cells were washed with PBS for three times and observed by the inverted fluorescence microscope.

***In vitro* DNA damage assay.** The DNA damage level of A549 cells were evaluated by single cell gel electrophoresis (comet assay). The cells were seeded in six-well plates and divided into six groups (negative control, positive control, MoS_2, TPZ, MoS_2@CG,

and MoS_2@CGTC NCR). After cultured for 24 h, the cells were treated with different samples. After co-incubated for 6 h, the cells were digested and washed with PBS for three times. 10 μL of cells suspension were added to 70 μL of 0.7% low melting point agarose. After denatured, electrophoresis, neutralized and stained, the DNA damage was observed by confocal microscope.

Bio-TEM assay. A549 cells were incubated with different samples for 12 h at standard condition. And then the cells were kept at 4 ℃ and immobilized for another 4 h using 2.5% glutaraldehyde. Next, the cells were dehydrated by graded ethanol, embedded, cut, and stained with uranyl acetate. Finally, the images of cell sections were observed on TEM (JEM-2100) at 120 kV.

***In vivo* antitumor experiment.** The A549 tumor-bearing male BALB/c nude mice were purchased from Cancer Hospital Chinese Academy of Medical Sciences. Mice drank with sterilized water, and the specific pathogen free (SPF) grade mouse food were purchased from Beijing Vitalriver Laboratory Animal Technology Co., Ltd. Mice were housed in cages under the thermostatic conditions with a whole day light/dark cycle. All procedures used in this experiment were compliant with the Chinese Association for Laboratory Animal Sciences and under protocols approved by the Key Laboratory for Biomedical Effects of Nanomaterials and Nanosafety, Institute of High Energy Physics. A549 tumor-bearing mice were randomly divided into the following five groups (n = 4): (i) 25 μL of PBS intratumoral (*i.t.*) injection as the control group, (ii) 25 μL of MoS_2@C *i.t.* injection for three times (4 mg mL^{-1}, once three days), (iii) 25 μL of TPZ *i.t.* injection for three times (0.4 mg mL^{-1}, once three days), (iv) 25 μL of

MoS_2@CG, and (v) 25 μL of MoS_2@CGTC NCR *i.t.* injection for three times (4 mg mL^{-1}, once three days), respectively. The body weight and tumor volume were recorded every 2 days.

Detection of GSH/GSSG ratio *in vivo*. The GSH/GSSG ratio *in vivo* were detected by GSH/GSSG assay kit (Beyotime). 10 mg of tumor tissues was milled into powder and added with 30 μL of protein solution M. After sufficient vortex, the mixed solutions were added another 30 μL protein solution M and fully homogenize with glass homogenizer. The samples were placed at 4 °C for 10 min and then centrifuged at 10000 rpm for 10 min at 4 °C. Finally, the supernatant was used for GSH and GSSG assay, and GSH/GSSG was detected according to the manufacturer's instructions.

Detection of ROS *in vivo*. 15 tumor-bearing male BALB/c nude mice were treated with TPZ, MoS_2@C, MoS_2@CG, MoS_2@CGTC NCR, and PBS as the control (n = 3 per group). The same dose of above samples (25 μL with a concentration of 4 mg mL^{-1}) was intratumorally injected into the mice. After 24 h, 50 μL of L-012 with a concentration of 50 mM as a chemiluminescence probe was intratumorally injected. The tumor ROS level was recorded through detecting the luminescence intensity of L-012 by using an IVIS Spectrum Imaging System (PerkinElmer, USA).

Blood and histology analysis. The blood samples were collected from the mice fundus artery in each group. 100 μL of blood solutions were treated with anticoagulant (potassium EDTA) for hematology analysis. After kept at 4 °C for 4 h and centrifuged, 200 μL of blood plasma samples were obtained from blood for biochemistry test. The blood analyses were accomplished at the Animal Department of Peking University

Medical Laboratory. In addition, the heart, liver, spleen, lung, kidney, and tumors were collected and fixed in 4% paraformaldehyde solution. Finally, all tissues were embedded, sectioned and stained by hematoxylin and eosin (H&E).

γ-H2AX immunohistochemical staining. The above tumor slices after paraffin embedding were stained with the γ-H2AX antibody (dilution 1:400), and the staining images were observed by the inverted fluorescence microscope.

HIF-1α immunohistochemical staining. First, the frozen sections of the tumors were incubated with HIF-1α antibody (dilution 1:800) and Alexa Fluor 488-conjugated goat anti-mouse IgG (SA00006-1) (dilution 1:200). Subsequently, cell nuclei were stained with 4',6-diamidino-2-phenylindole (DAPI). The staining mages were observed by the inverted fluorescence microscope.

HP2-kit immunohistochemical staining. In addition, to further confirm the aggravated hypoxia ability during the treatment, tumors in each group were excised at 2 h after intravenous (*i.v.*) injection of pimonidazole hydrochloride (60 mg/kg) (Hypoxyprobe-1 plus kit, Hypoxyprobe Inc.) and then sliced into slices for further staining. To detect the pimonidazole, antipimonidazole mouse monoclonal antibody (dilution 1:200, Hypoxyprobe Inc.) was used as primary antibody for further staining and fluorescence imaging. Finally, the staining images were observed by the inverted luminescence microscope.

Statistical Analysis. The obtained experimental results were expressed as means ± standard deviation (SD) and the statistical difference analysis was evaluated by

Student's t-test (two-tailed). P values of less than 0.05 (*) were considered statistically significant.

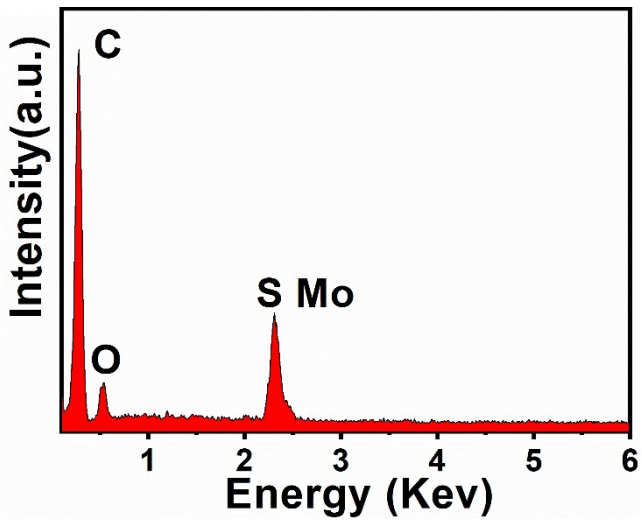

Fig. S1 EDS of MoS_2@C NSs.

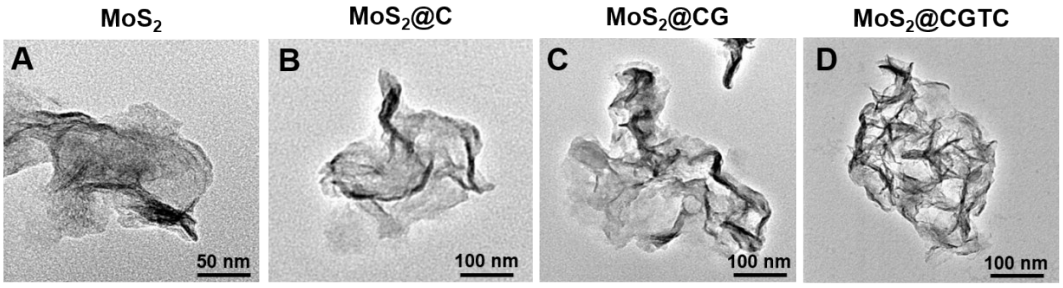

Fig. S2 TEM images of (A) MoS_2, (B) MoS_2@C, (C) MoS_2@CG, and (D) MoS_2@CGTC, respectively.

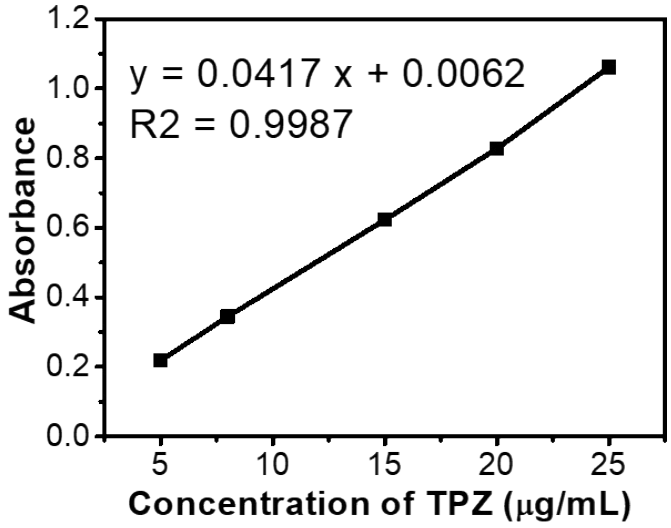

Fig. S3 The concentration-dependent standard curve of TPZ.

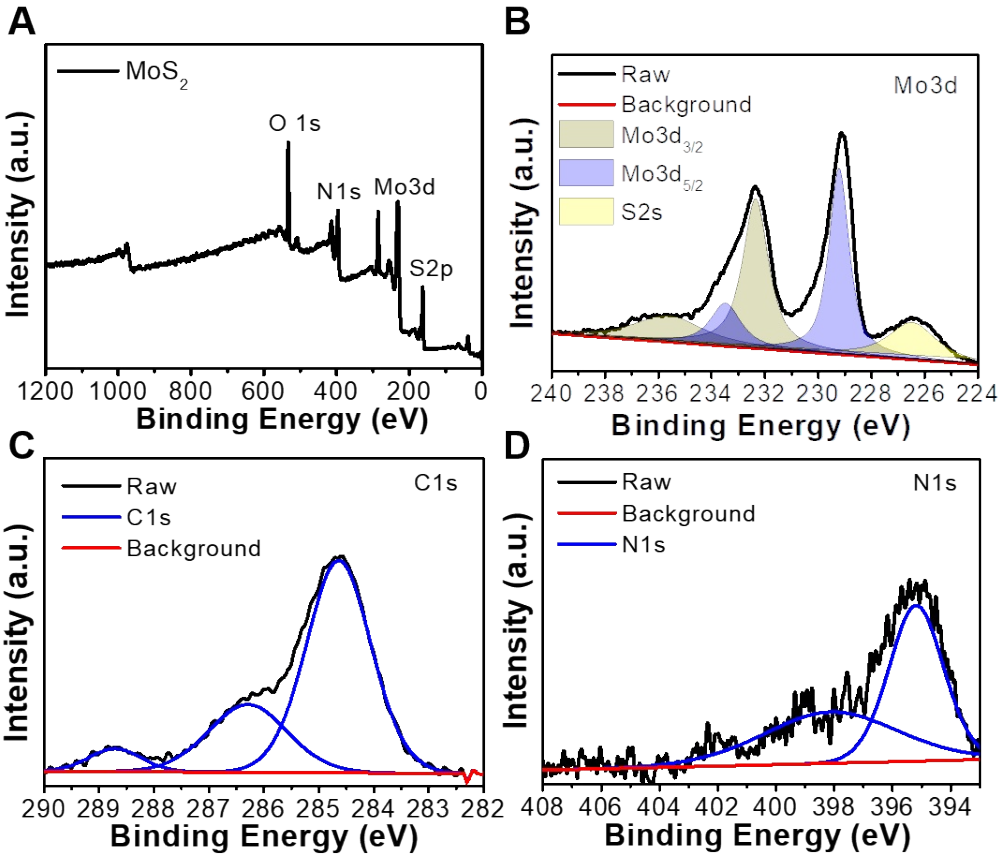

Fig. S4 (A) XPS full spectrum of MoS_2 NSs. (B) Deconvolution of high-resolution (B) Mo3d, (C) C1s, (D) N1s XPS spectra of MoS_2 NSs.

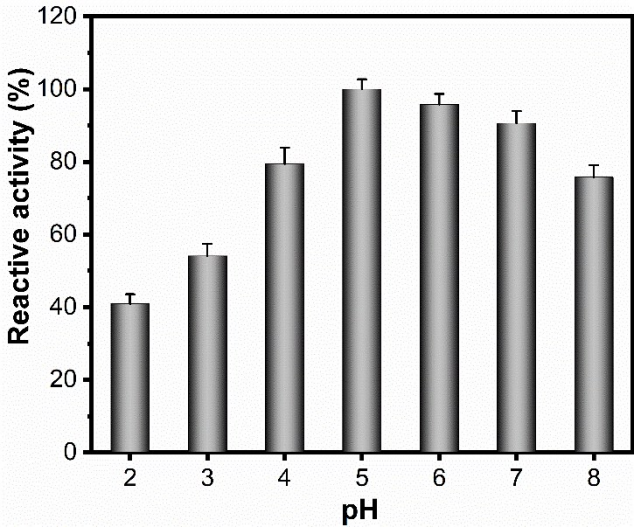

Fig. S5 Relative catalytic activity of GOx after being incubated with different pH values for 2 h.

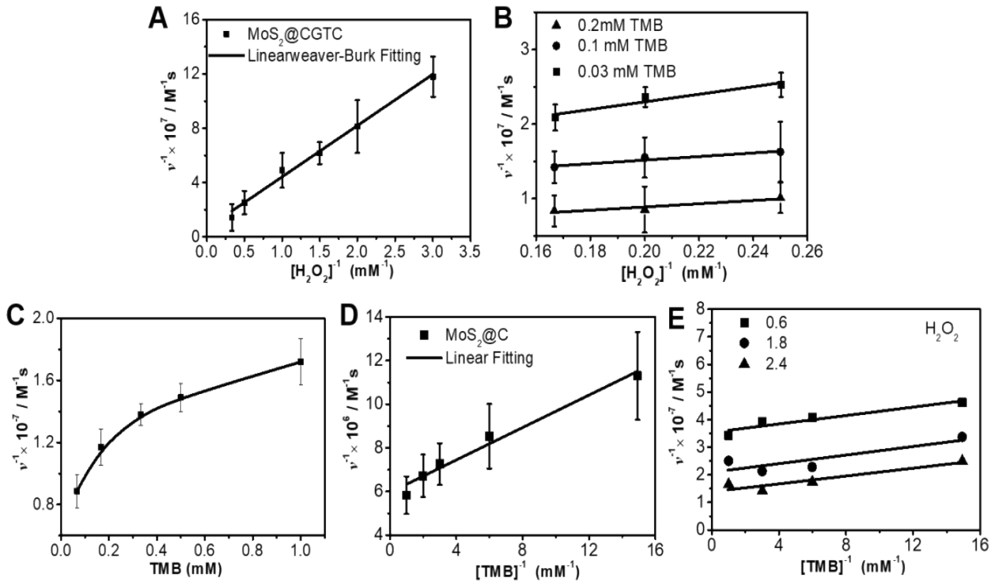

Fig. S6 (A) Lineweaver–Burk plotting of MoS_2@CGTC under different H_2O_2 concentrations. (B) Double reciprocal plots of activity of MoS_2@CGTC with the concentration of one substrate TMB fixed and vice versa. (C) Michaelis–Menten kinetics and (D) Lineweaver–Burk plotting of MoS_2@CGTC NSs under different TMB concentrations. (E) Double reciprocal plots of activity of MoS_2@CGTC NSs with the concentration of one substrate H_2O_2 fixed and vice versa. The error bars represent the standard deviation of three measurements.

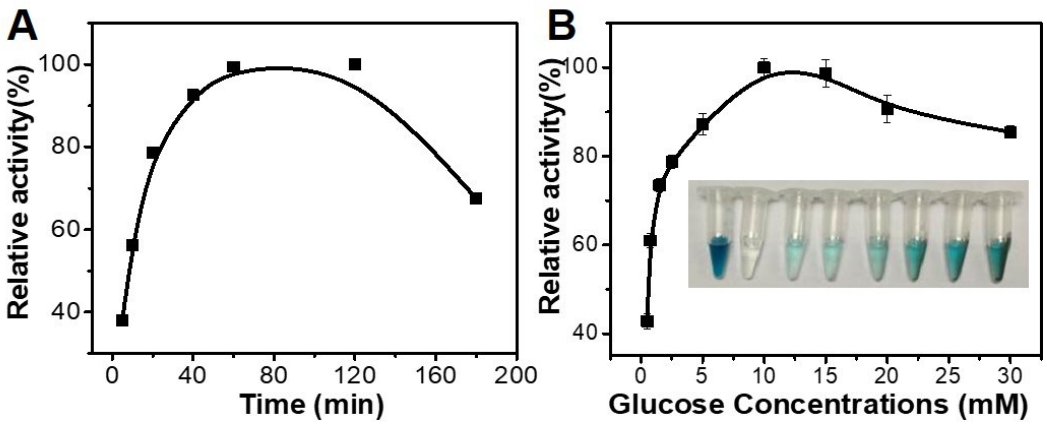

Fig. S7 Peroxidase-like catalytic activity of MoS_2@CGTC NCR depends on (A) Time and (B) Glucose concentrations. The error bars in (B) represent the standard deviation of three measurements. The inset in and (B) was typical photograph of the glucose colorimetric solutions with different concentrations.

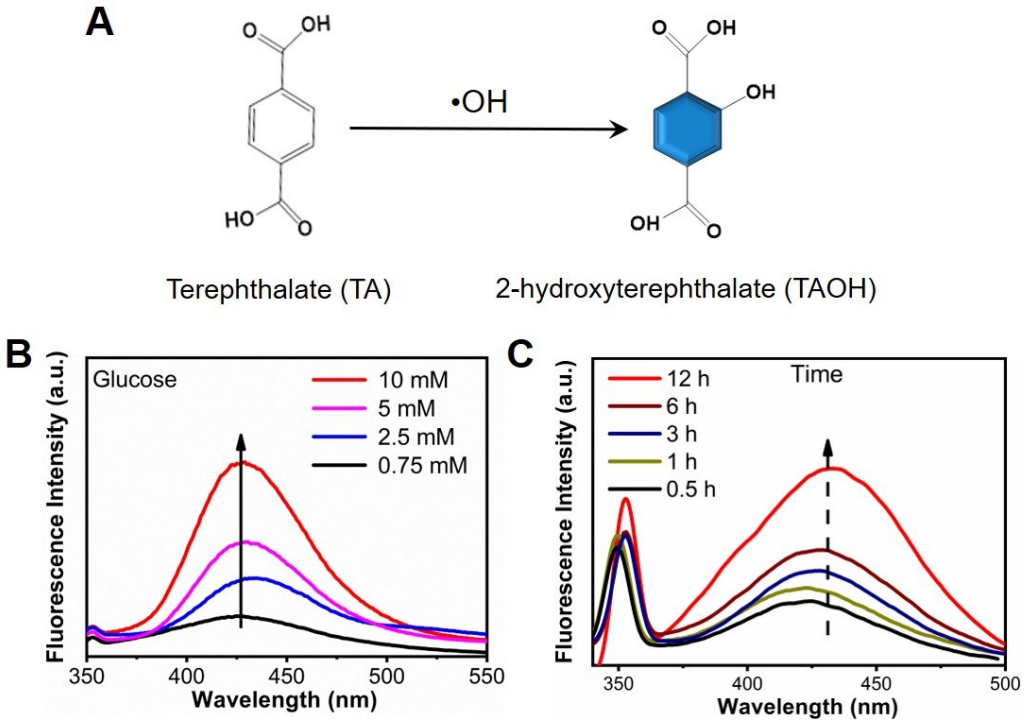

Fig. S8 (A) Nonfluorescent compound terephthalic acid (TA) reacts with hydroxyl radical (•OH) to form stable fluorescent 2-hydroxy-TA (TAOH) to detect the •OH generated by decomposition of H_2O_2. Fluorescence spectra of TAOH induced by MoS_2@CGTC NCR with (B) different glucose concentrations (0.75, 2.5. 5 and 10 mM) and (C) different time (0.5, 1, 3, 6, and 12 h).

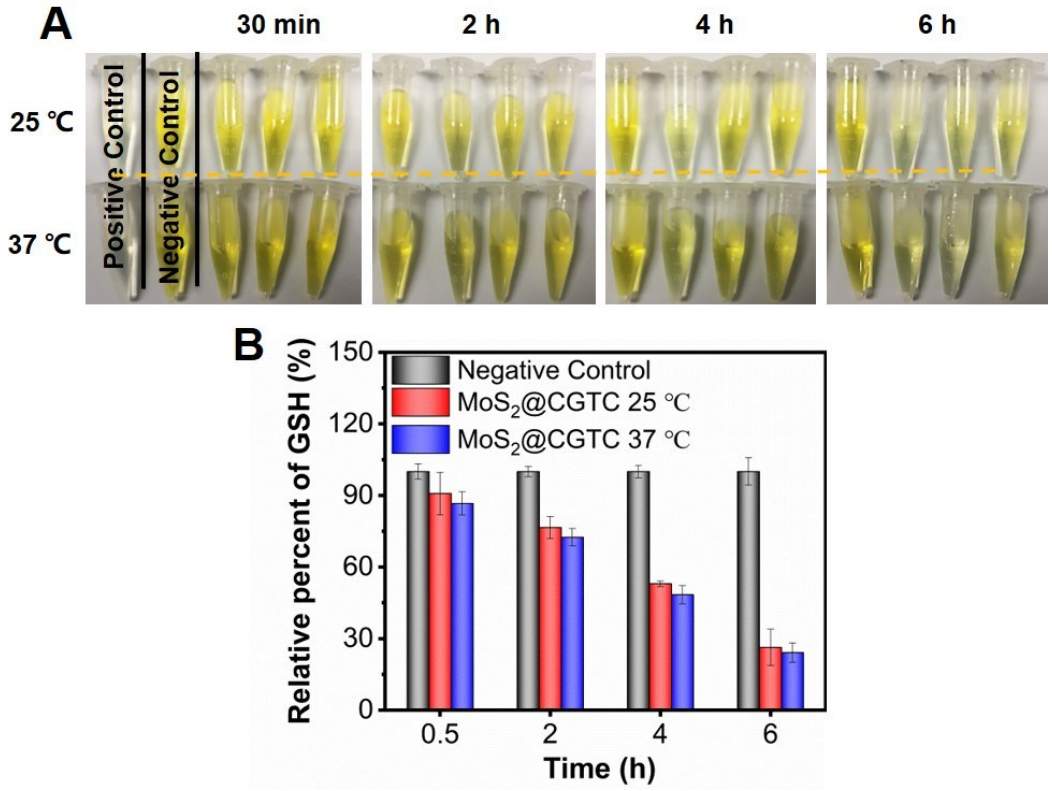

Fig. S9 Visual observation of color change after GSH treatment of MoS_2@CGTC NCR with different time under 25 and 37 ℃ water bath, respectively, detected by the Ellman's assay. We found that temperature has less influence on the GSH oxidation behavior, but the MoS_2@CGTC NCR exhibited remarkable time-dependent GSH oxidation behavior. H_2O_2 (1.0 mM) was used to oxidize GSH (1.0 mM) and as a positive control. (B) Relative percent of GSH after different treatments. The error bars represent the standard deviation from the three times of repeated experiment.

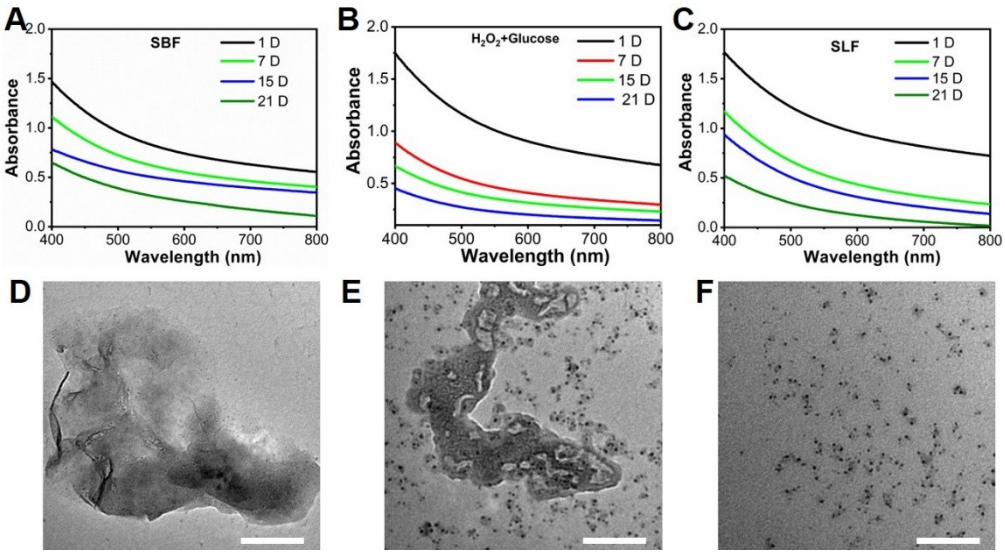

Fig. S10 Biodegradation behaviors of MoS_2@CGTC NCR. UV-vis-NIR spectra (A-C) and TEM images (D-F) of MoS_2@CGTC NCR after biodegradation in (A, D) Simulated body fluid (SBF), (B, E) H_2O_2 + Glucose and (C, F) Simulated lysosome fluid (SLF) for varied durations (1, 7, 15, and 21 days). Scale bar = 100 nm

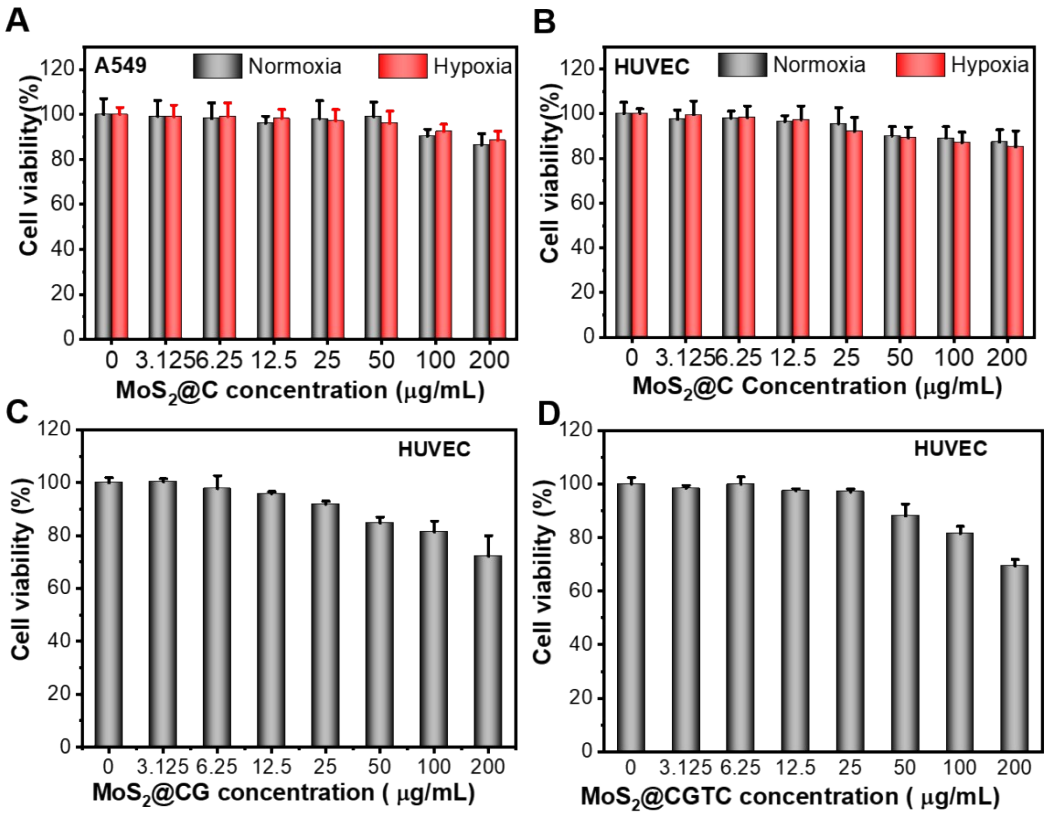

Fig. S11 Cell viabilities of (A) A549 and (B) HUVEC incubated with different concentrations of MoS_2@C for 24 h under normoxia and hypoxia conditions. Cell viabilities of HUVEC incubated with different concentrations of (C) MoS_2@CG and (D) MoS_2@CGTC NCR under low glucose and normoxia conditions. Error bars represent standard deviation for n = 6.

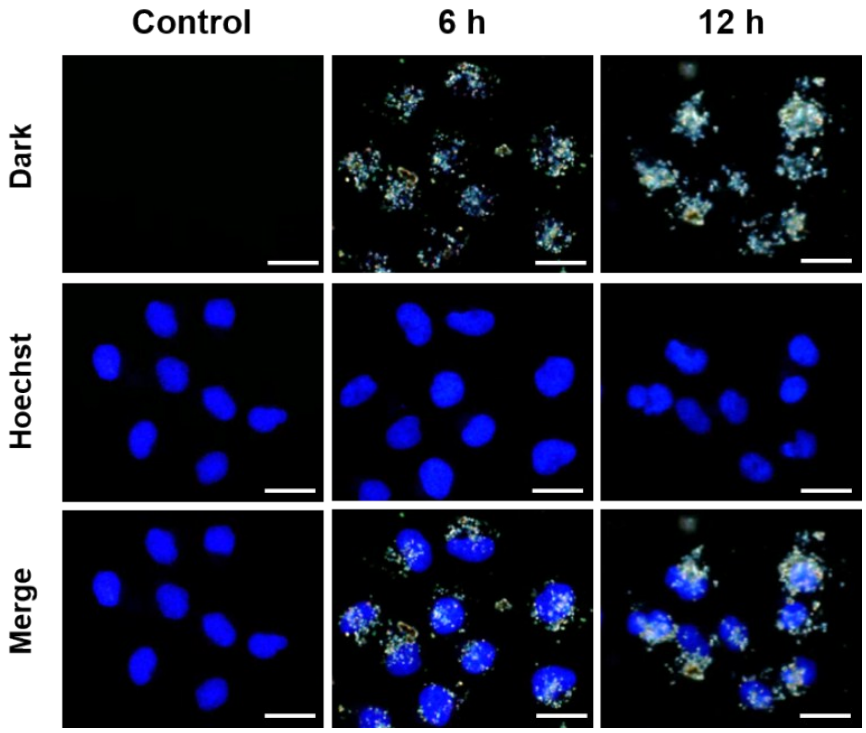

Fig. S12 Dark-field optical microscopy images of A549 cells incubated with MoS_2@C (30 μg/mL) for 6 h and 12 h. Cell nucleus were stained with Hoechst 33342. Scale bar = 10 μm.

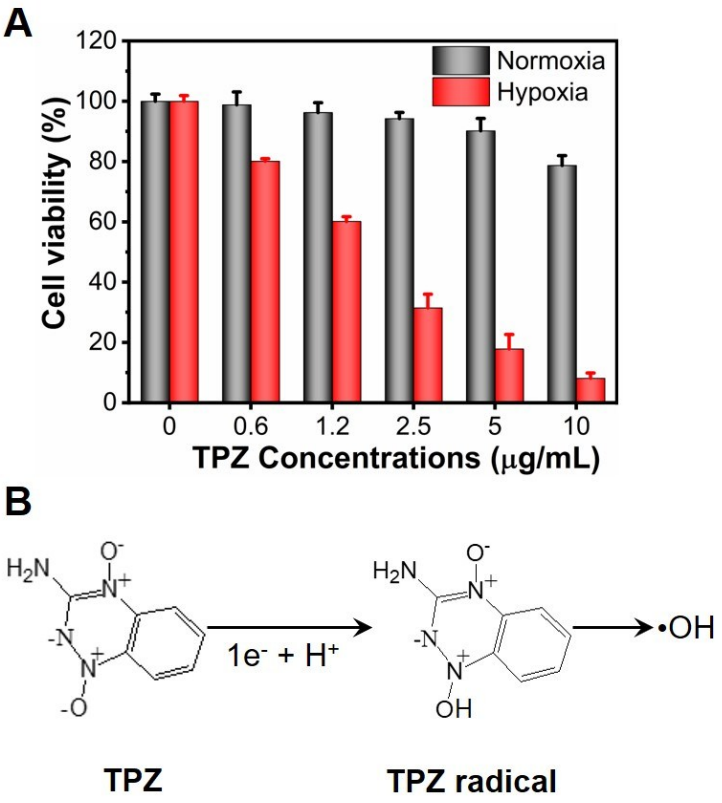

Fig. S13 (A) Cell viabilities of A549 treated with varied concentrations of free tirapazamine (TPZ) in normoxia and hypoxia environments for 6 h. (B) The mechanism by which TPZ selectively killed hypoxic cells.

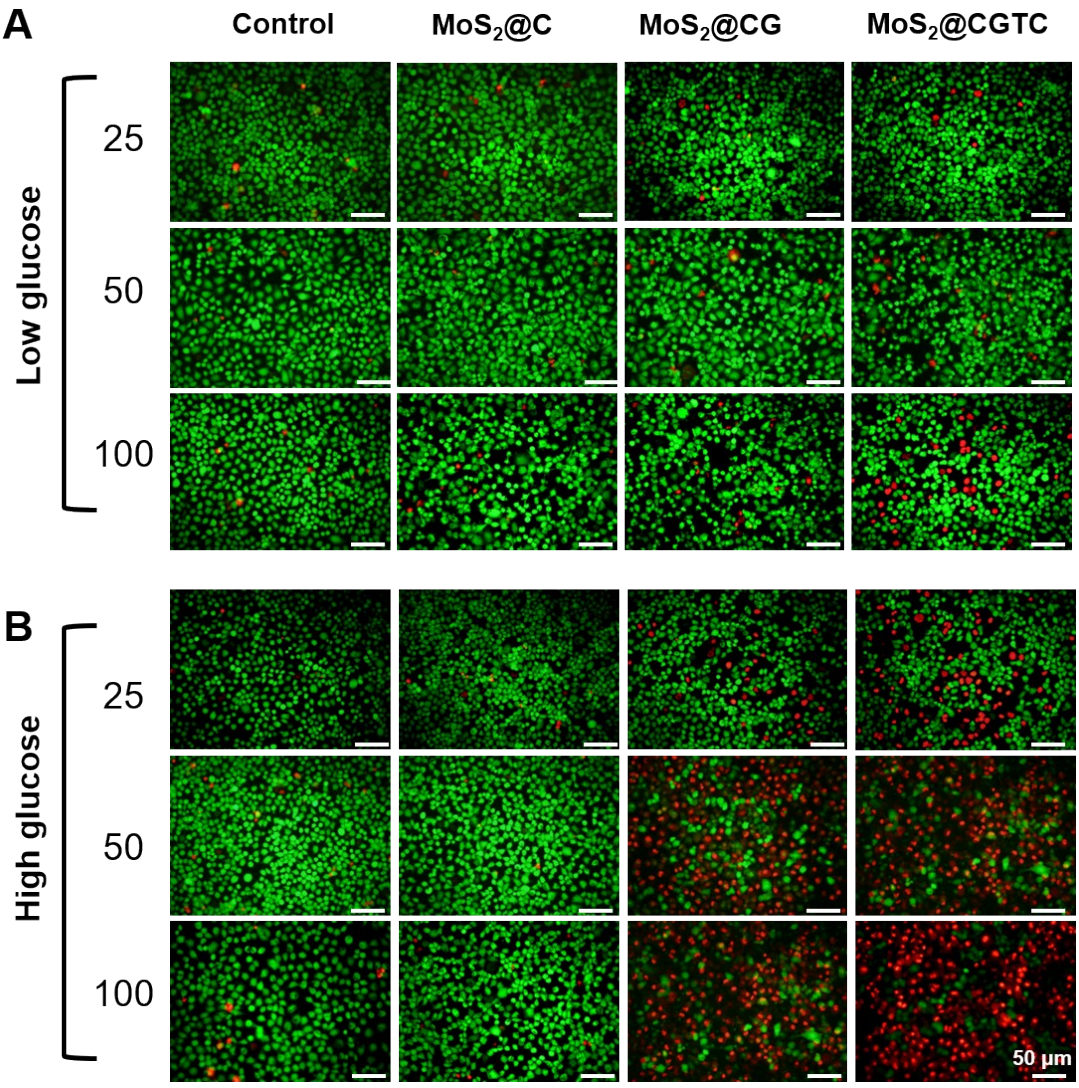

Fig. S14 Representative CLSM live/dead cell fluorescence images of the A549 cells stained with Calcein-AM (live cells, green fluorescence) and PI (dead cells, red fluorescence) after treated with (A) low glucose and (B) high glucose for 10 h.

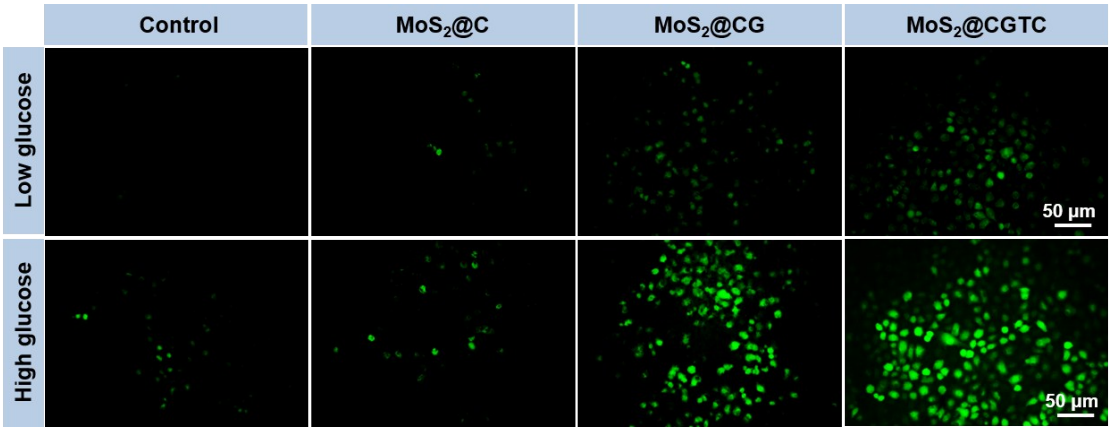

Fig. S15 Fluorescence images for A549 cells staining with DCFH-DA (a ROS fluorescent probe, green) after different treatments under low/high glucose and normoxia condition.

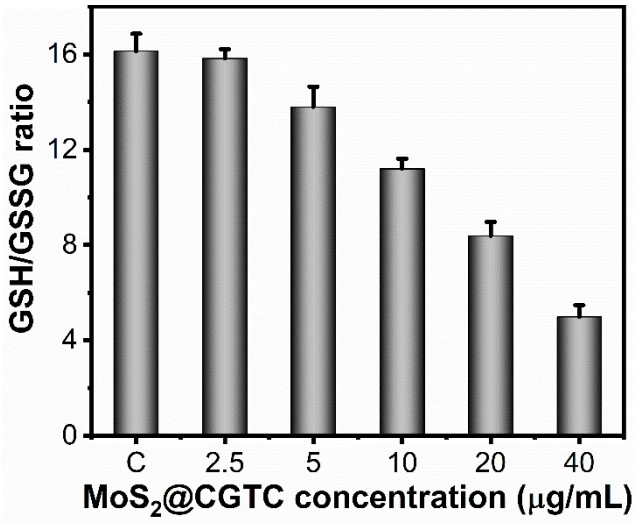

Fig. S16 Intracellular GSH/GSSG ratio in A549 cells after treated with different concentrations of MoS_2@CGTC NCR for 12 h.

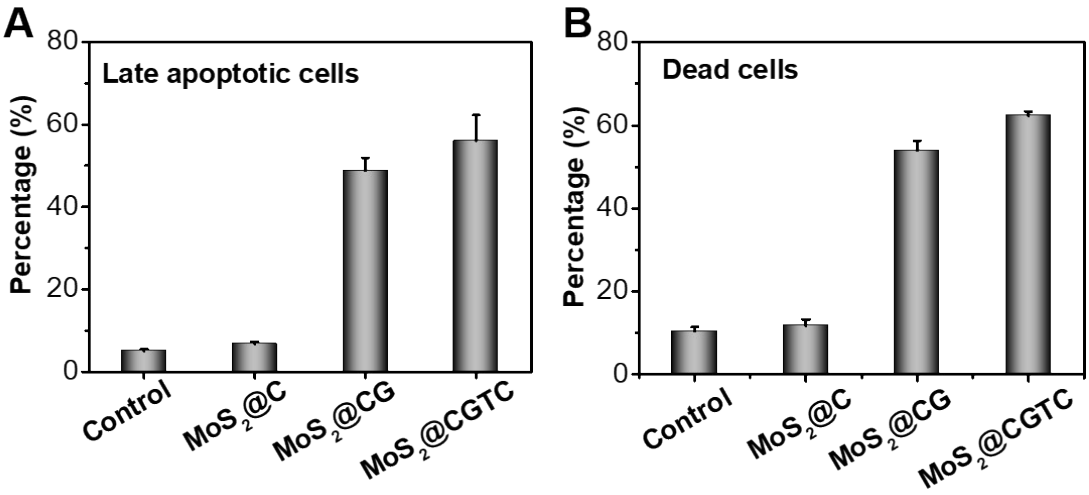

Fig. S17 Statistical analysis of percentage of the corresponding (A) late apoptosis and (B) dead cells under different treatments. Error bars represent standard deviation for n = 3.

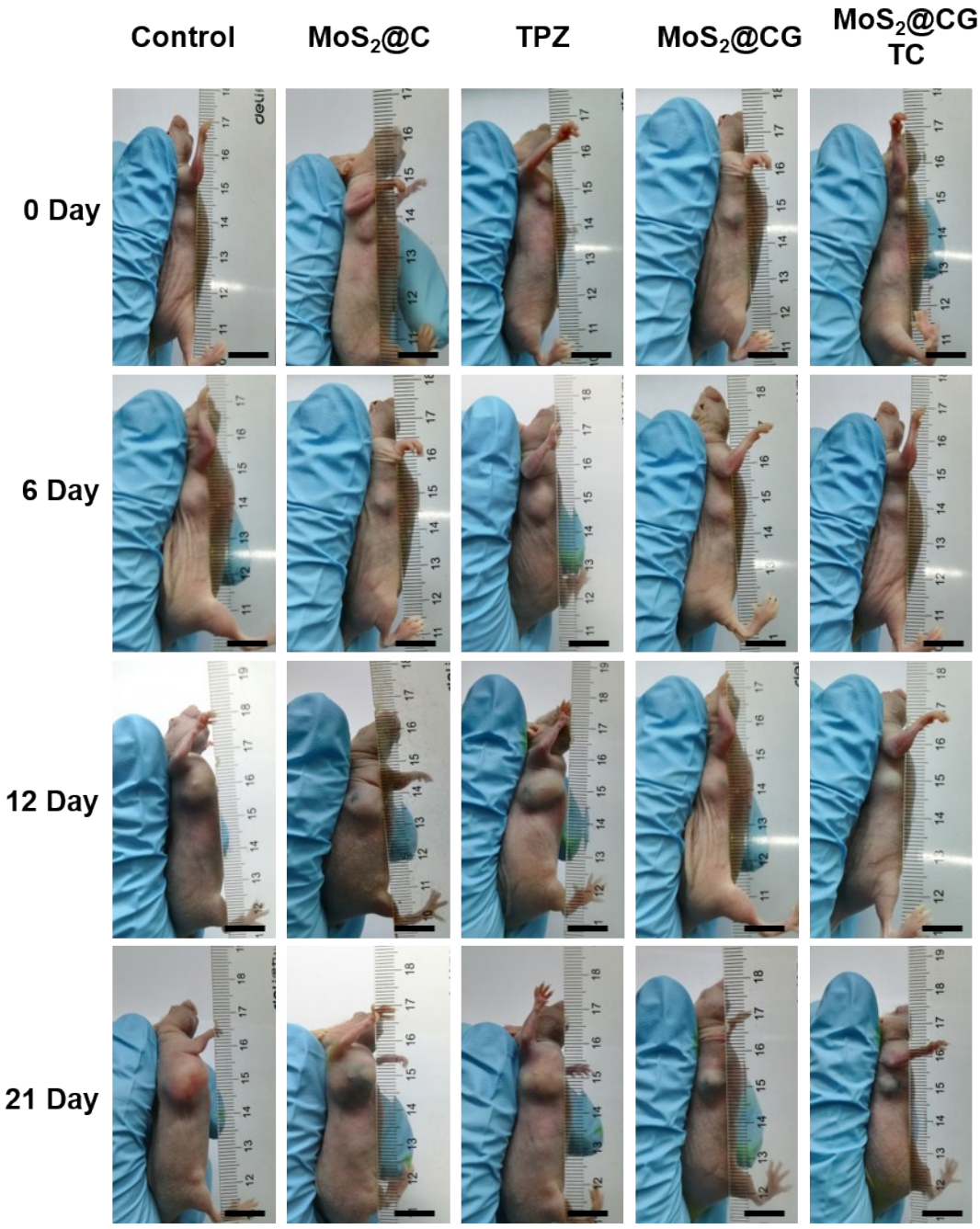

Fig. S18 Digital photographs of different groups of mice at 0, 6, 12, and 21 days after different treatments. Scale bar = 1.50 cm.

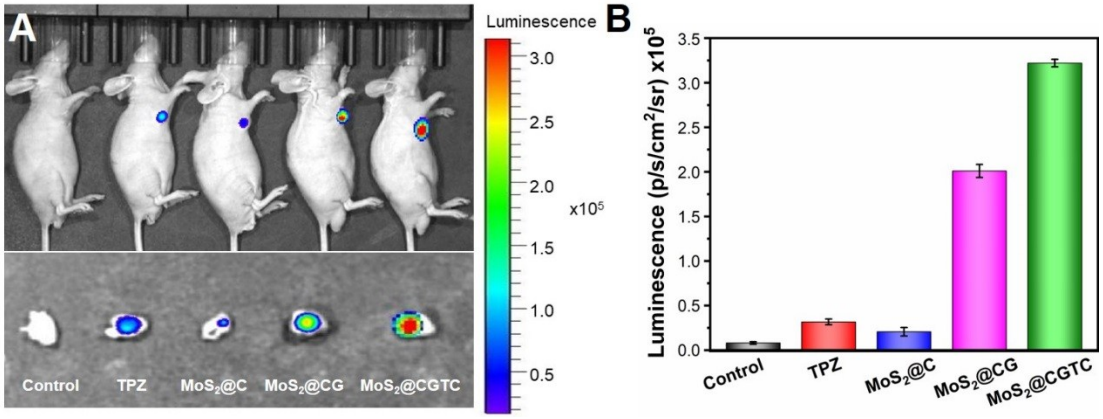

Fig. S19 Detection of the generation of ROS *in vivo* using ROS probe L-012. (A) Luminescence images of mice after different treatments in the following groups: control, TPZ, MoS_2@C, MoS_2@CG, and MoS_2@CGTC NCR. (B) The normalized luminescence intensities in different groups. Error bars represent the standard deviations (n = 3).

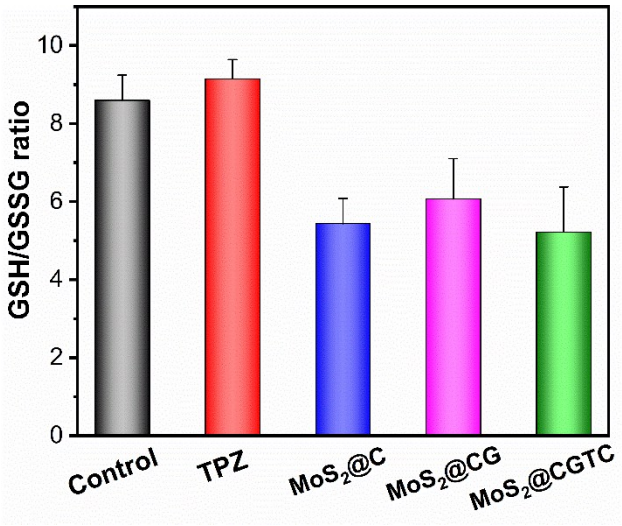

Fig. S20 GSH/GSSG ratio changes of tumor tissues after different treatments.

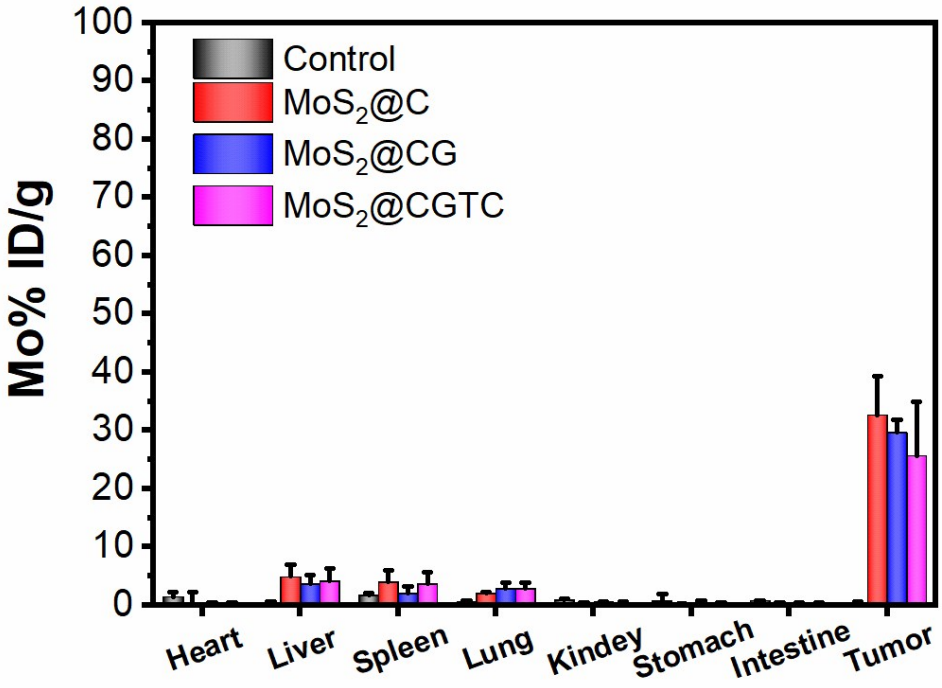

Fig. S21 The biodistribution of Mo (% administrated dose (ID) of Mo per gram of tissues) in main tissues and tumor after intratumorally injected with MoS_2@C, MoS_2@CG, and MoS_2@CGTC NCR for 21 days. Error bars represent standard deviation for n = 4.

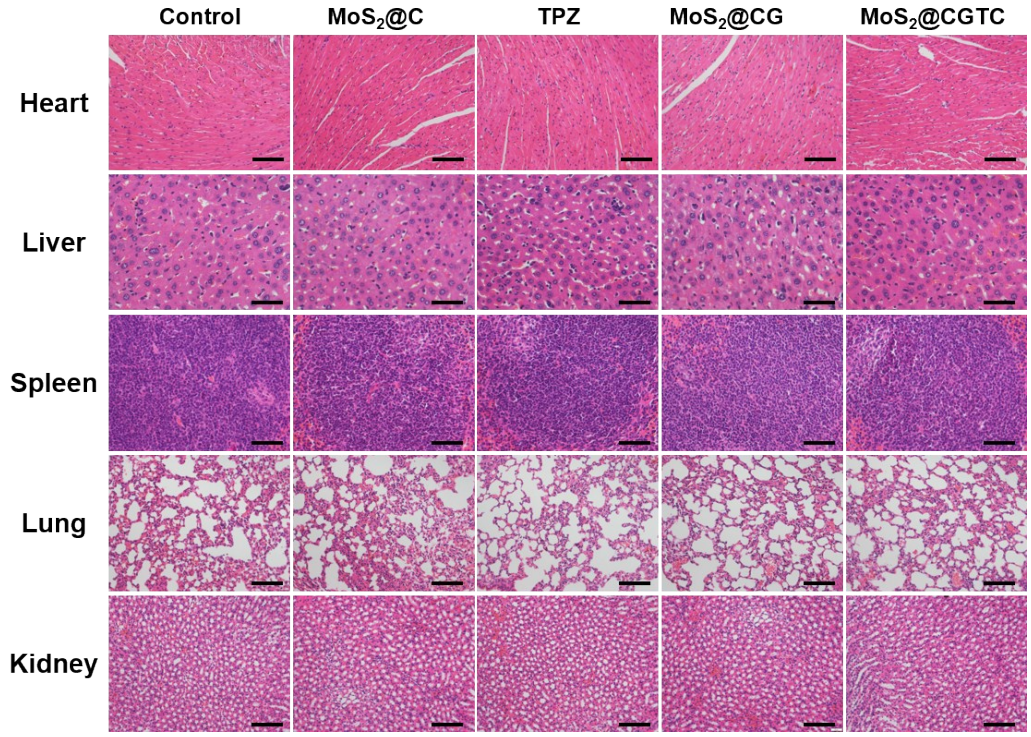

Fig. S22 Representative H&E stained images of the main organs collected from A549 tumor-bearing nude mice on the last day after various administrations. Scale bar = 100 μm.

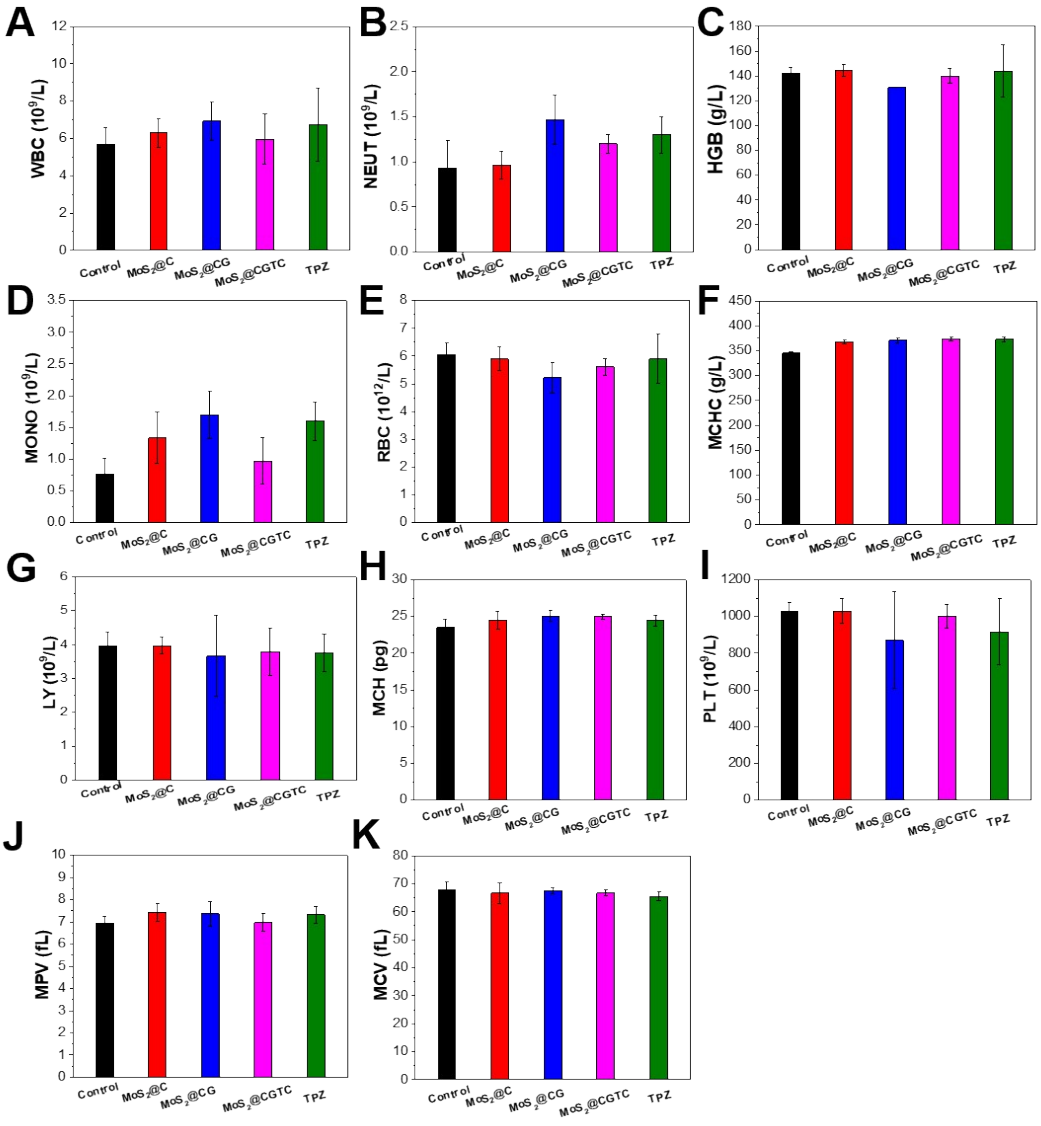

Fig. S23 Blood hematology analysis of the mice after different treatments on the 21st day. The results show the (A) white blood cell (WBC), (B) neutrophil count (NEUT), (C) hemoglobin (HGB), (D) monocytes count (MONO), (E) red blood cell (RBC), (F) mean corpuscular hemoglobin concentration (MCHC), (G) lymphocyte (LY), (H) mean corpuscular hemoglobin (MCH), (I) platelets (PLT), (J) mean platelet volume (MPV), and (K) mean corpuscular volume (MCV) in each group. Error bars represent standard deviation for n = 4.

Table S1. Comparisons of the apparent Michaelis-Menten constant (K_m) and maximum reaction rate (V_{max}) in different systems.

Nanozyme	Substrate	K_m (mM)	V_{max} (10^{-7} Ms^{-1})
HRP[1]	TMB	0.43	1.00
HRP[1]	H_2O_2	3.70	0.87
MoS_2@CGTC NCR	TMB	0.06	1.69
MoS_2@CGTC NCR	H_2O_2	6.57	1.74

Reference

1. L. Gao, J. Zhuang, L. Nie, J. Zhang, Y. Zhang, N. Gu, T. Wang, J. Feng, D. Yang, S. Perrett and X. Yan, *Nat. Nanotechnol.*, 2007, **2**, 577.